Emittance of a Reverse-Extracted Beam from the TITAN RFQ Trap

Timothy Blais, Aaron Gallant & Ernesto Mané

We measured the transverse emittance of a bunched reverse-extracted beam of ^{133}Cs ions from TITAN's RFQ ion trap cooler and buncher, using an Allison-type emittance scanner inserted into the polarizer beamline. Both the cooling time and the amount of gas flowing through the trap were varied, with scans taken for each setting. The beam was found to be converging with a width (FWHM) ranging from 6-8 mm and an RMS emittance ranging from 1.94-2.48 π mm mrad. However, a measurement anomaly, which seems to have suppressed much of the positive-divergence beam current, may necessitate a repeat of the measurement with a modified setup.

July 2010

1. The RFQ Trap

An RFQ (Radio Frequency Quadrupole), or Paul trap, is an ion trap that uses time-varying electric fields to trap a beam of ions in a confined space. Shown schematically in Figure 1, it consists of a segmented linear arrangement of quadrupole electrodes, whose polarity is constantly being switched by a square radio-frequency signal. This high-frequency switching creates a pseudopotential that contains the ions inside the trap, confining them an oscillatory motion along both axes of the quadrupole. The ions can then be confined in the axial dimension by floating the quadrupole segments at different DC voltages to create a local potential well.

The purpose of the TITAN Paul trap is to act as a cooler and buncher of incoming ion beams. To accomplish this, the entire trap is floated at high voltage so that an incoming ion beam loses most of its kinetic energy upon entry. Once trapped, the ions are cooled by elastic collisions with a hydrogen or helium buffer gas that constantly flows through the trap. This damps out the oscillatory motions of the ions, and they pool in the trap's potential well. To extract the ions, the outer wall of the potential well is lowered and the ion bunch is “kicked” out of the trap. The well can be placed at the front end of the trap if bunched beam is being forward-extracted and sent through to the rest of the TITAN experiment, or at the back end if, as in this case, the beam is to be reverse-extracted to the polarizer beamline. This is the first RFQ cooler-buncher in the world capable of producing reverse-extracted beams, making our emittance measurement the first of its kind.

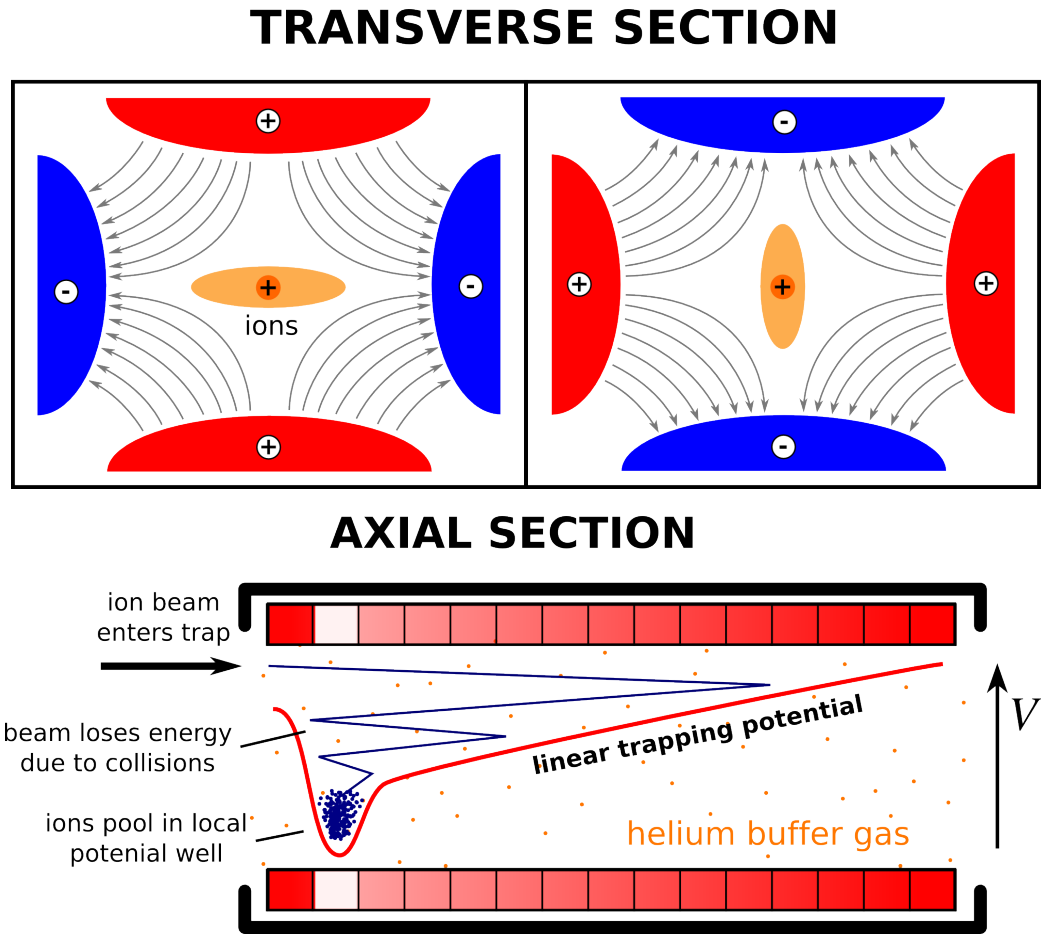

Figure 1: Transverse and axial sections of the RFQ trap. The grey lines in the top figure represent electric field lines, while the red line in the bottom figure is the trapping potential along the z-axis of the RFQ.

2. Theory Of Emittance Measurement

Roughly speaking, the emittance of a particle beam is a measure of its position- and energy-spread. The full emittance is proportional to the 6-dimension phase-space volume occupied by some given fraction of the beam [1]. However, this can usually be separated into three two-dimensional phase-space areas, each dealing with the spread of the beam along a single spatial axis. The longitudinal emittance, along the beam's axis of propagation, quantifies the longitudinal position- and velocity-spread of the beam, while the two transverse emittances give information about the cross-section of the beam and its tendency to focus or defocus [1]. The phase space for the transverse axes is usually plotted as position vs. trajectory angle (or divergence), and transverse emittances (which are areas of this phase space) are typically given in units of π mm mrad [1].

An emittance plot is a phase-space diagram that shows the beam current at each position and divergence value (see figures 2 and 3 for examples). The shape of this plot depends on the history of the beam, but for an RFQ it is generally elliptical for transverse emittances [1]. The shape and orientation of this ellipse can be used to determine certain characteristics of the beam, such as whether it is converging or diverging. (For more information on the parametrization of the emittance ellipse see Stockli, 2006 [1].) In this case, the area of a fit-ellipse on the emittance plot that contains a certain fraction of the beam-current can be used as a measure of the beam's emittance. An alternate measure is the RMS emittance, which is useful for non-elliptical beams and uses a weighted RMS average of all phase-space points. It is given by the formula [1]:

$$E^{x}_{RMS} = \sqrt{\langle x^2 \rangle \cdot \langle x'^2 \rangle - \langle x \cdot x' \rangle^2} \qquad (1)$$

where x is position, x' is trajectory angle and each angle bracket is an average over all measured points, weighted by their beam-current intensity.

There are many different types of emittance detectors, but for this measurement an Allison-type detector was used. This is a one-dimensional emittance scanner that uses thin slits and a pair of deflector plates to selectively detect particles with a particular angle of approach. As shown in Figure 2, the beam particles passing through the front slit have a distribution of x-momenta. However, only those with a very specific angle of entry are deflected so that they pass through the second slit and and are detected in the Faraday cup. By changing the potential difference across the deflector plates, we can

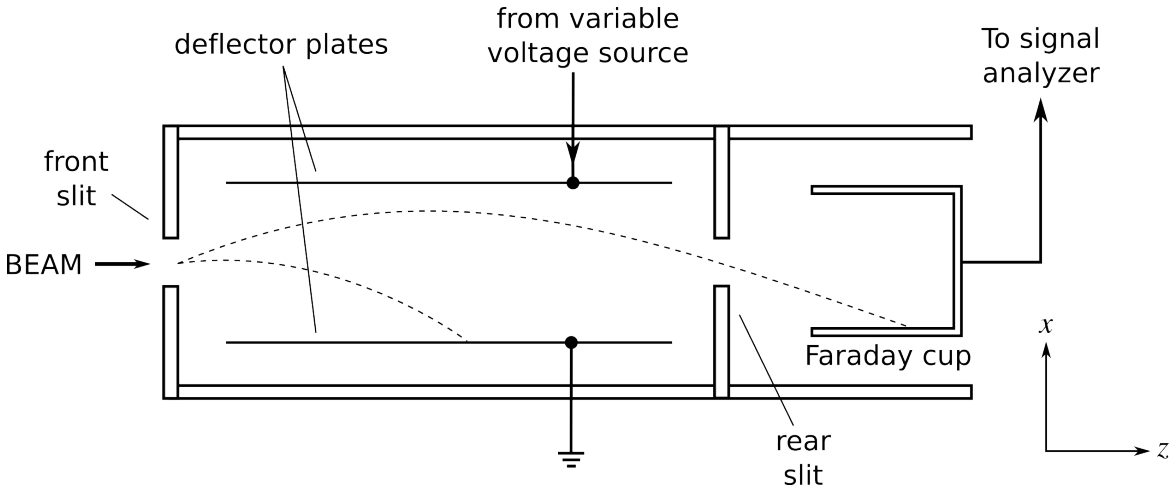

Figure 2: Diagram of the Allison emittance scanner.

Constant	*Symbol*	*Value*
Slit width	s	0.025 mm
Plate separation	g	4 mm
Effective plate length	D	65.85 mm
Beam accelerating voltage	ϕ	20 kV

Table 1: Experimental constants and their values

therefore scan the entire angular distribution of the beam [2]. If one assumes negligible energy spread and a constant field between the plates, the equation relating the angle of the accepted particles to the deflector voltage can be derived with simple kinematics. It is given by [2]:

$$x' = \frac{V}{\phi}\frac{D}{4\mathrm{g}} \tag{2}$$

where the x' is the angle from the horizontal (in radians), V is the deflector potential and all other constants are defined in Table 1. The meter is attached to a computer-controlled stepper motor that allows the position of the slits to be adjusted precisely. By performing sweeps of the deflection voltage at various positions along the beam profile, this allows a full scan of the x-p_x phase-space of the beam. While this approach only enables us to measure the beam's emittance in a single transverse direction, its behaviour in the orthogonal direction should be qualitatively and quantitatively similar.

3. Measurement

The beam used for this measurement comes from the TITAN stable ion source, and contains mostly ^{133}Cs ions, although lighter alkali metals are also present in lower quantities. It is bunched by TITAN's Paul trap, while being cooled with helium buffer gas, before being reverse-extracted to the site of the measurement which is just upstream from the photomultiplier in the polarizer beamline. At the measurement site, the ions are traveling at an energy of 20keV, in bunches with a frequency of 100Hz.

The data-taking process was largely automated using a LabVIEW interface. However, the power-supply used to bias the deflector plates required a manual polarization switch to go from positive and negative voltages. Because of this, each scan was taken in two data sets, one with positive and one with negative deflection voltages. The two sets were then glued together to obtain the full emittance plot. The measurement was taken across 13 positions spaced 1mm apart, with the deflection voltage scanned in 1-V increments from -15V to 15V at each point.

Our first measurement of the beam emittance was taken using a beam that had undergone a cooling time of 5 ms inside the RFQ trap with a buffer gas flow of 10 sccm. Having achieved a successful plot, we decided to tweak some of the parameters of the beam to determine their effect on the measured emittance. We first reduced the cooling time inside the RFQ to 2ms and then increased it to 9ms, taking new measurements for each. We next returned to a 5ms cooling time and adjusted the flow rate of buffer gas into the RFQ down from 10sccm to 6sccm and then to 8sccm, in order to determine what effect a reduced flow, which effectively reduces the gas pressure in the trap, would have on the emittance. The resulting emittance plots are shown in figures 3-12. Each scan is plotted both as a simple histogram and as an interpolated contour plot, which were generated by running the data through two different analysis programs. The histogram scale is in total number of ions detected. The curve overlaying the histogram plot in each case is the best-fit RMS ellipse—that is, an ellipse with its area equal to the RMS emittance.

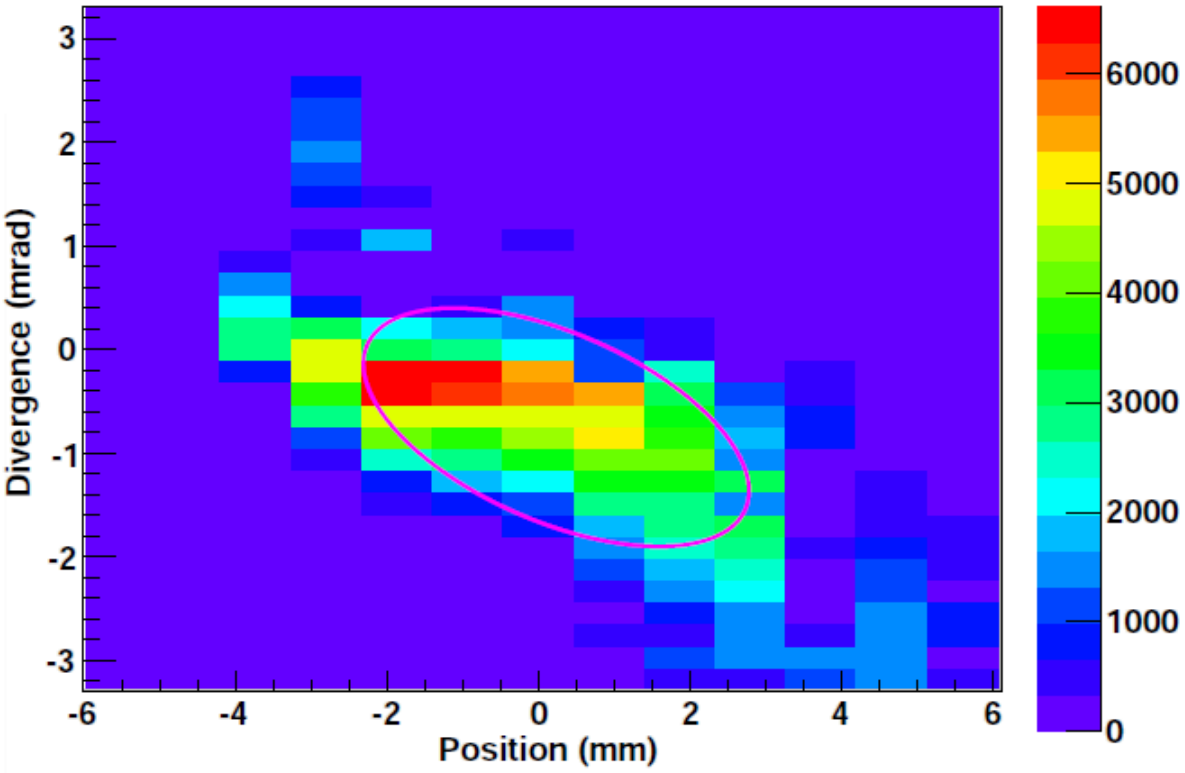

Figure 3: Histogram emittance plot and RMS ellipse at 5ms cooling time and gas flow of 10sccm

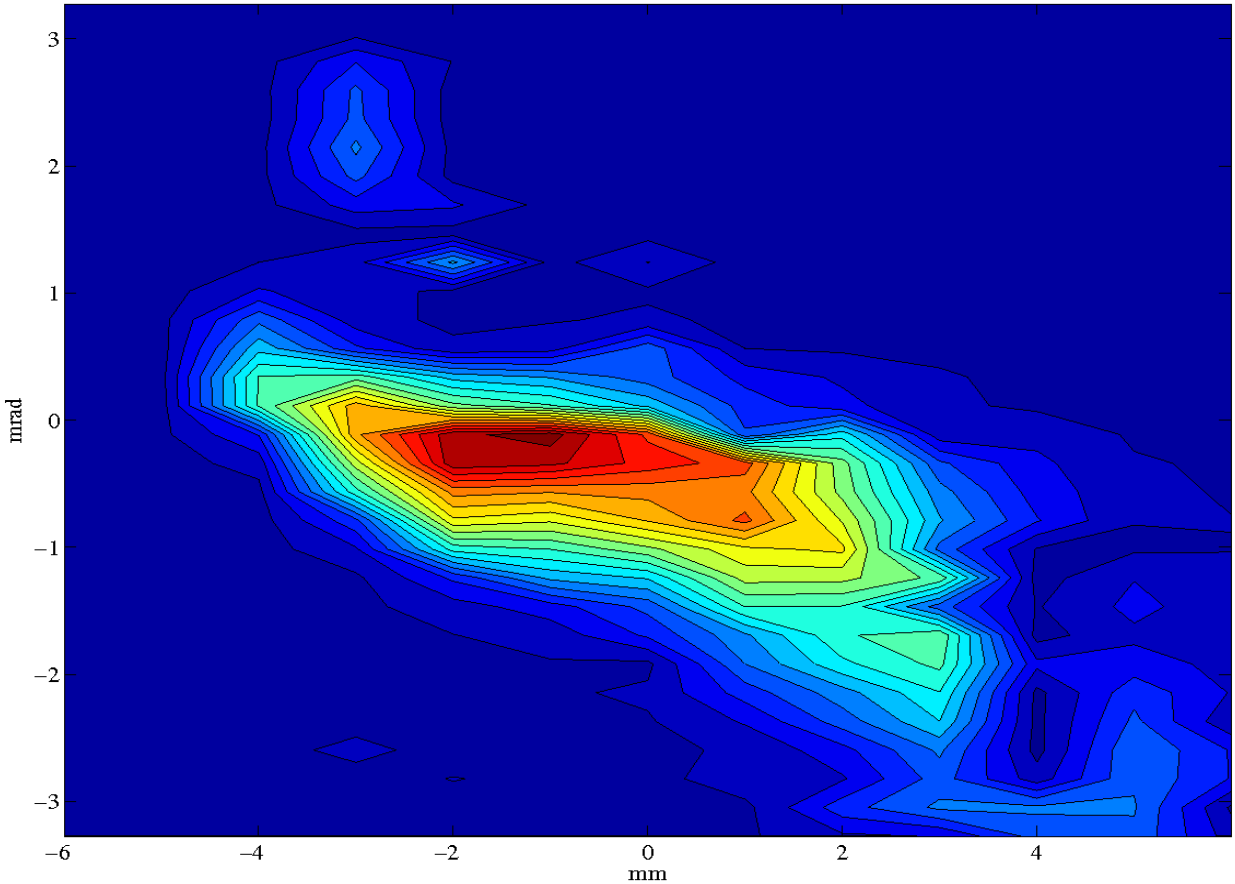

Figure 4: Contour emittance plot for the beam at 5ms cooling time and gas flow of 10sccm

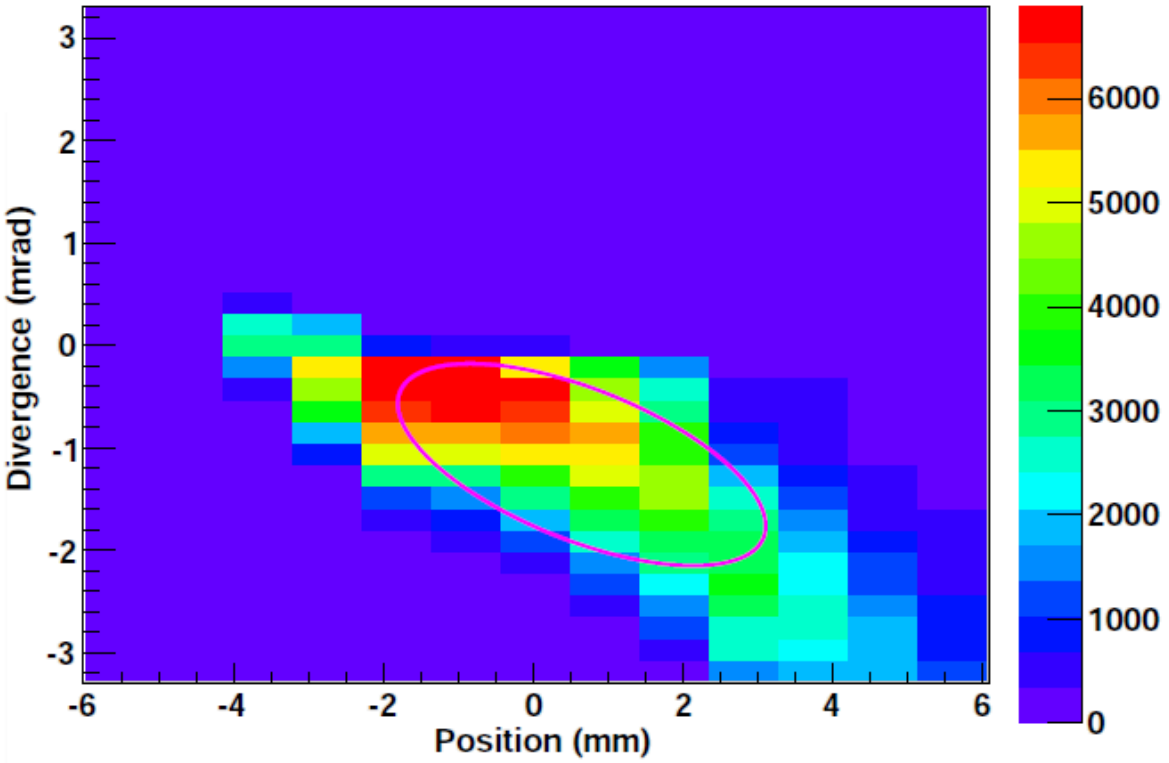

Figure 5: Histogram emittance plot and RMS ellipse at 2ms cooling time and gas flow of 10sccm

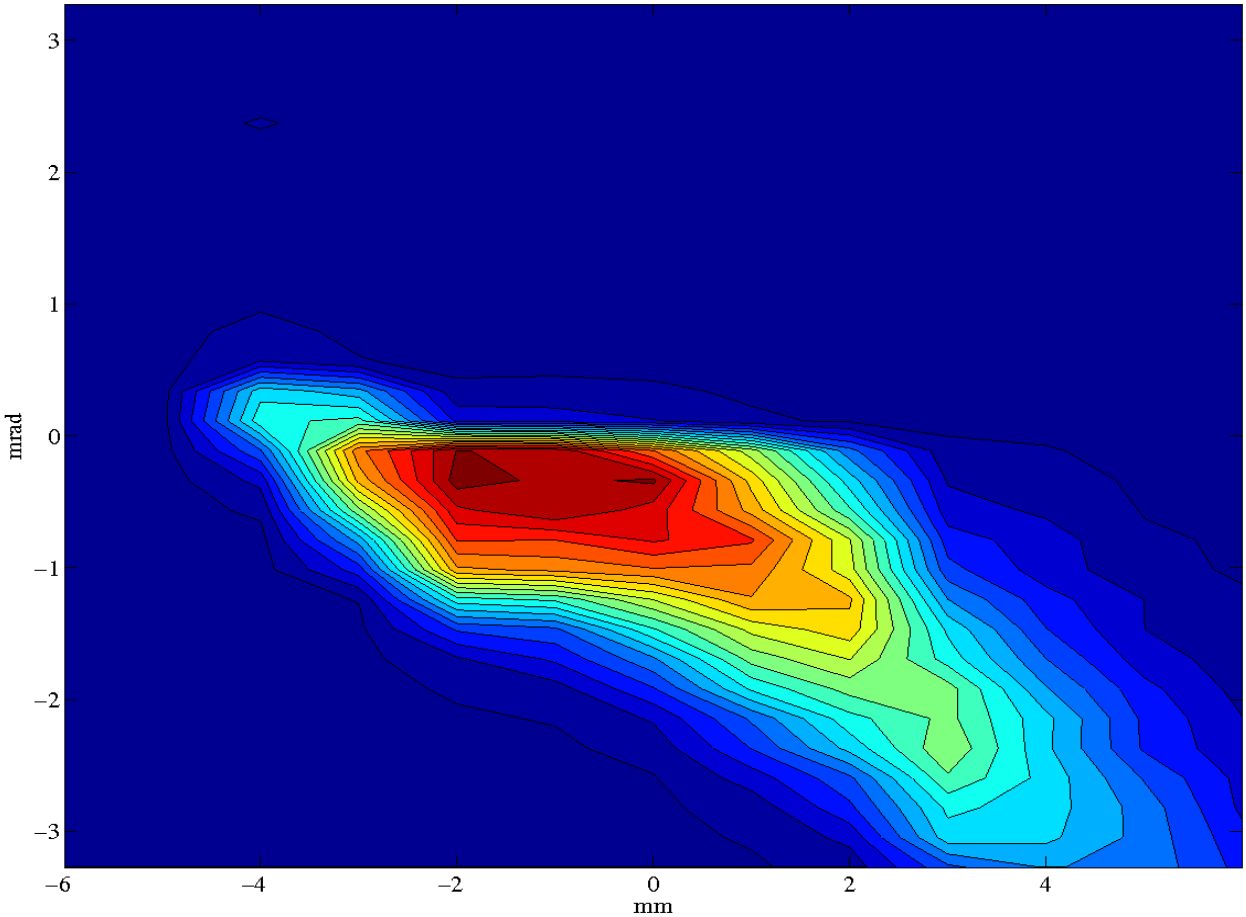

Figure 6: Contour emittance plot for the beam at 2ms cooling time and gas flow of 10sccm

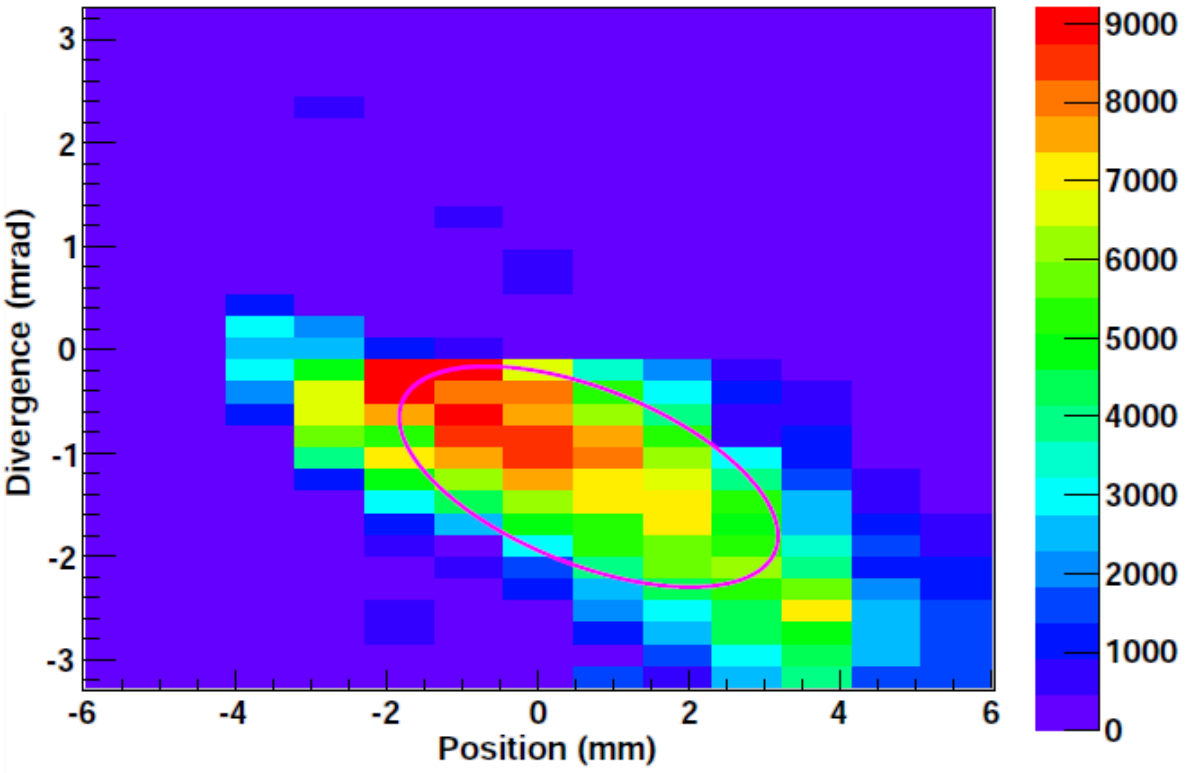

Figure 7: Histogram emittance plot and RMS ellipse at 9ms cooling time and gas flow of 10sccm

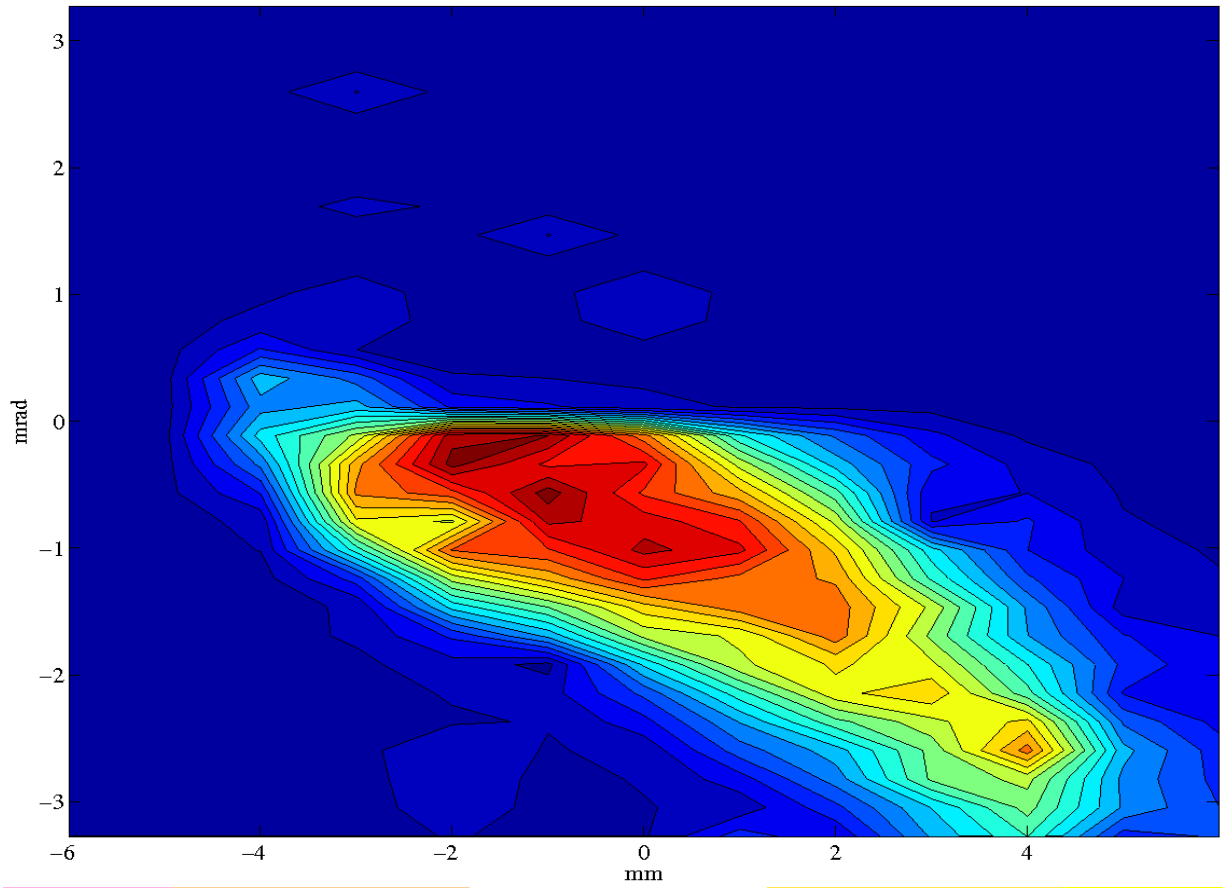

Figure 8: Contour emittance plot for the beam at 9ms cooling time and gas flow of 10sccm

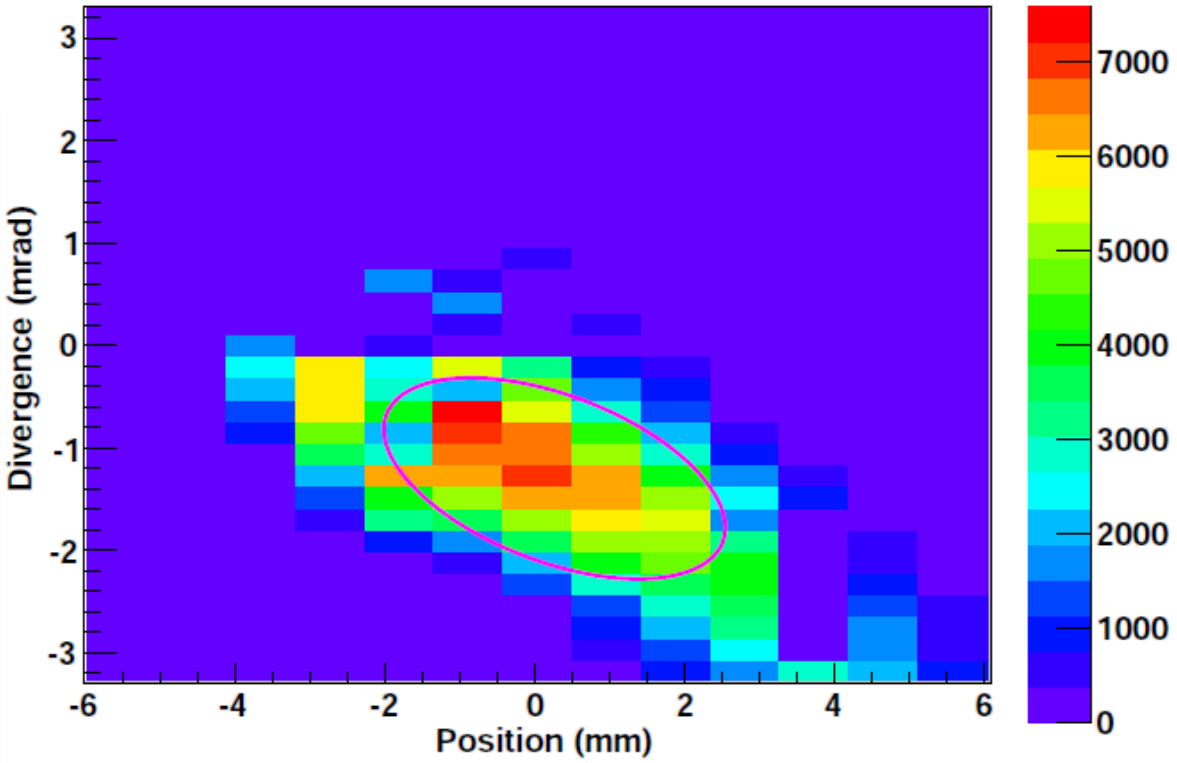

Figure 9: Histogram emittance plot and RMS ellipse at 5ms cooling time and gas flow of 6sccm

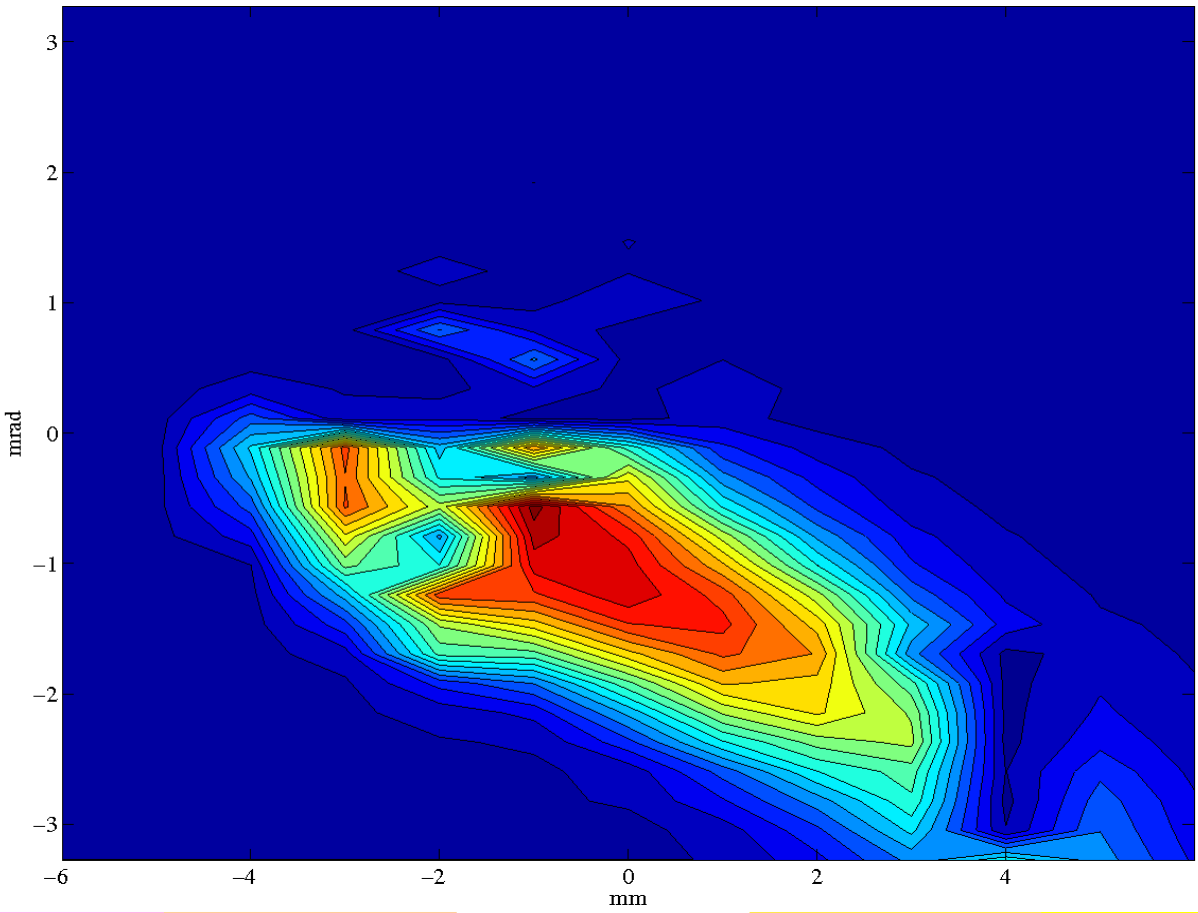

Figure 10: Contour emittance plot for the beam at 5ms cooling time and gas flow of 6sccm

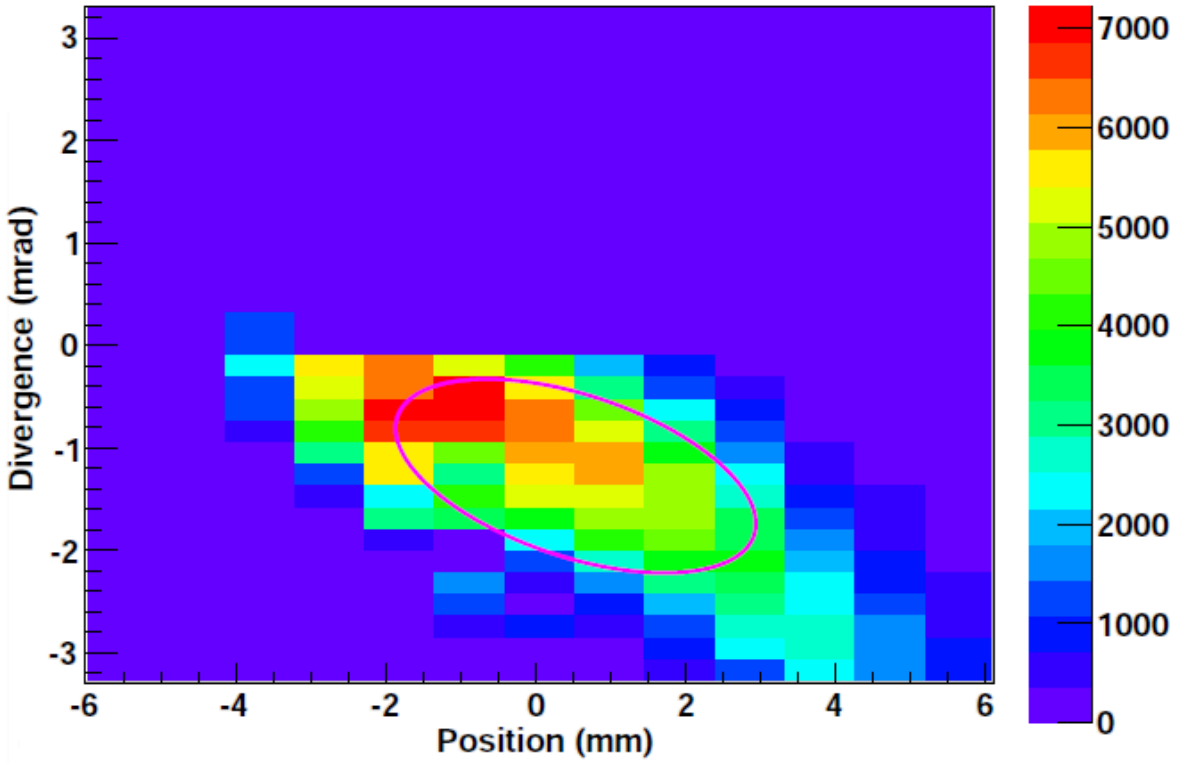

Figure 11: Histogram emittance plot and RMS ellipse at 5ms cooling time and gas flow of 8sccm

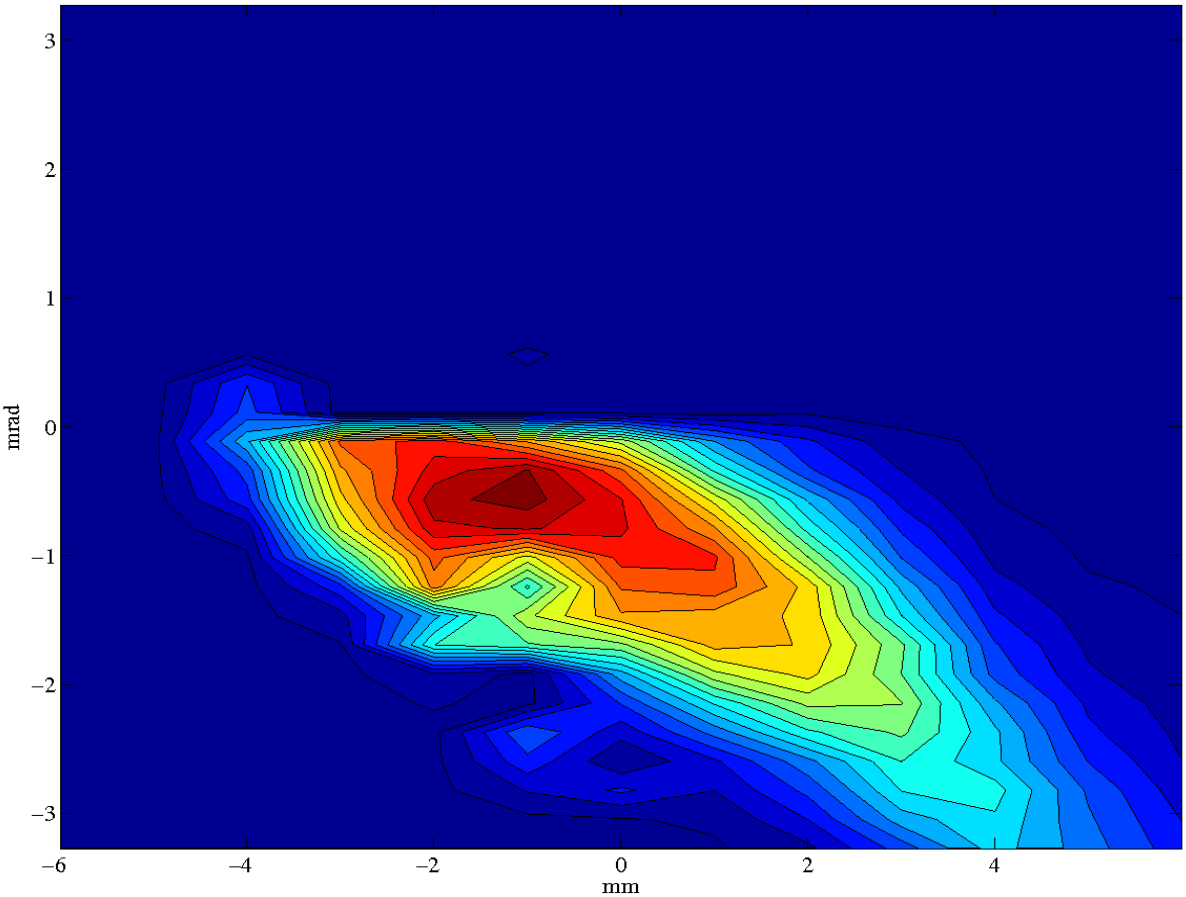

Figure 12: Contour emittance plot for the beam at 5ms cooling time and gas flow of 8sccm

4. Analysis

While in general the plots have the expected elliptical shape on the lower half of the plane, they all seem to be cut off in the upper half, which offsets the best-fit ellipse from the apparent maximum of the plot. This will be discussed further below. The best-fit ellipses of all the plots show a negative slope, indicating a converging beam.

Figure 13 shows the beam profile in position space for each of the five data sets, taken by integrating the beam current across all divergences at each slit position. It reveals the beam to have the expected, roughly Gaussian shape, with a FWHM ranging from 6-8 mm. Even given that the beam is converging this may be slightly too wide for the purposes of upcoming experiments, in which case the quadrupole optics in the polarizer beamline must be adjusted to better focus the beam. It should be noted that emittance is an invariant characteristic of the beam when being focused by standard optics, so such an adjustment s not change the overall emittance; only the shape of the ellipse.

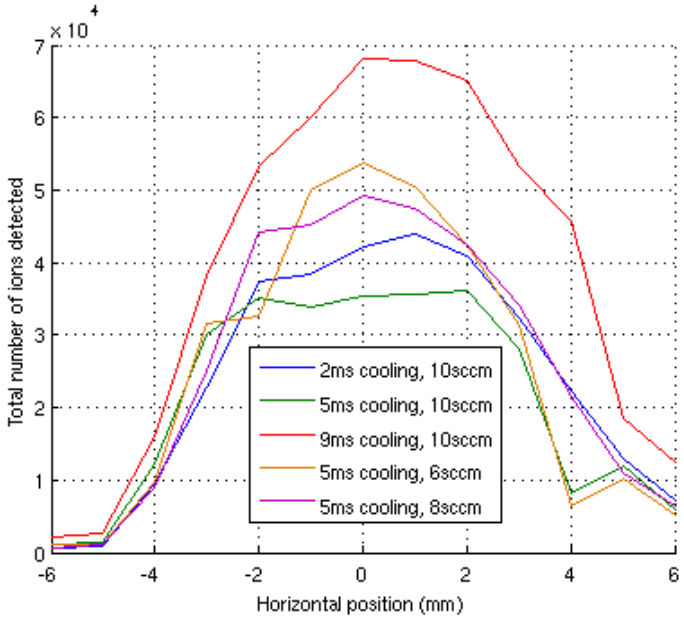

Figure 13: Position-space beam profiles

In figure 14, the same raw data is integrated over positions to give a profile in momentum space. This reveals what was already visible looking at the emittance plots: a 1-dimensional discontinuity as the data pass from negative to positive divergence. This indicates something systematically wrong with the switch from negative to positive voltages. It is possible that the actual voltage of the power supply has some constant offset from its readout at low voltages, so that when reading zero it may actually have some finite voltage. In such case a polarity change would cause a change in the deflection voltage by several volts, leading to a discontinuity. However, assuming the actual emittance of the beam to be fairly symmetric—which it should be—requires this offset to be on the order of tens of volts, which seems to disagree with the fact that the spectrum peaks near zero on the negative side. Another possibility is that the ions in the beam with positive velocity are being selectively blocked, perhaps somewhere inside the detector, though this too seems strange given the tiny deflection angles being worked with. If the beam is in fact being clipped, we may be systematically underestimating our emittance measurements by up to a factor of 2.

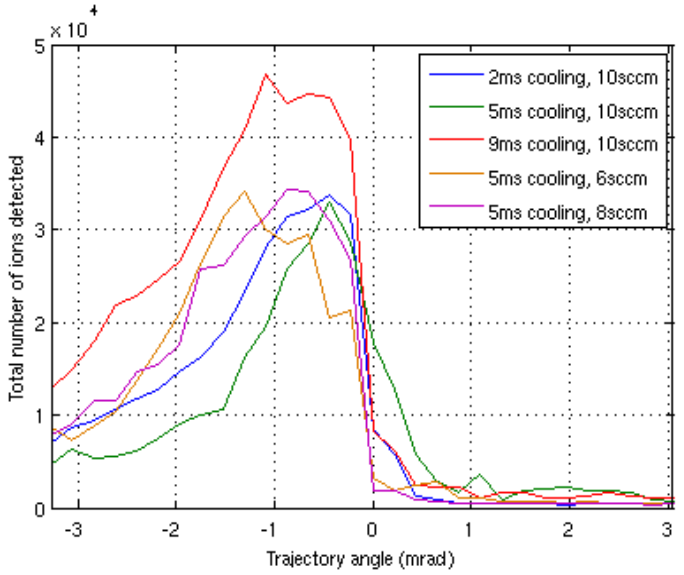

Figure 14: Momentum space beam profiles

Cooling Time (ms)	Gas Flow (sccm)	$\varepsilon_{39\%}$ (π mm mrad)	$\varepsilon_{99\%}$ (π mm mrad)	ε_{RMS} (π mm mrad)
2	10	1.520(47)	16	1.94(1)
5	6	1.507(46)	23.8	1.97(1)
5	8	1.592(48)	21.6	1.98(1)
5	10	1.589(55)	28.2	2.48(1)
9	10	1.859(56)	30.6	2.29(1)

Table 2: Emittances for the varied experimental conditions. Digits in parentheses represent the statistical error on the last digits of the measurement.

Table 2 tabulates several different measures of the emittance as taken from the five sets of data. The 39% and 99% emittance values were calculated with elliptical fits using Rick Baartman's "Emitmat" Matlab program, which also produced the emittance contour plots. The RMS emittance and its error were calculated using a ROOT C++ script that was also used to make the histogram emittance plots.

Figure 15 shows the elliptical fit emittances of all five plots as they scale with the fraction of the beam found outside the ellipse. These data seem to indicate that, in general, it is the the beams that underwent *less* buffer-gas collisions (i.e. those that saw shorter cooling times and/or reduced gas pressure) that have the *lowest* emittance. Unfortunately, these data were not produced with error estimates, making it difficult to determine whether the effect is real. However, figures 16 and 17, which show the dependence of the RMS emittance on the two varied parameters, indicate the same trend that less collisions result in general in lower emittances. Should this turn out to be a valid trend it is the opposite of what might be expected, and indeed why this should be the case is not clear. Nevertheless, it would be good news for the actual experimental conditions, in which the cooling time is expected to not exceed 1ms. What is not certain, unfortunately, is whether these results can be considered valid given that we are clipping the upper half of the beam; it could well be that the dominating factor is not the actual emittance of these beams, but simply how much of them was cut off.

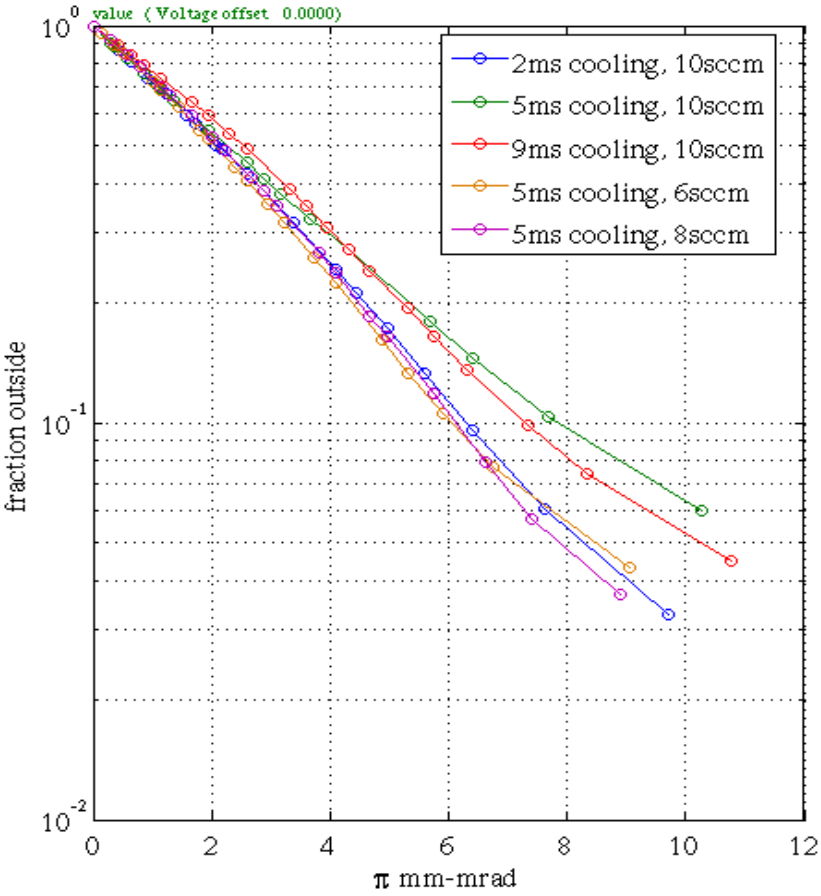

Figure 15: Fractional emittances for the various cooling conditions.

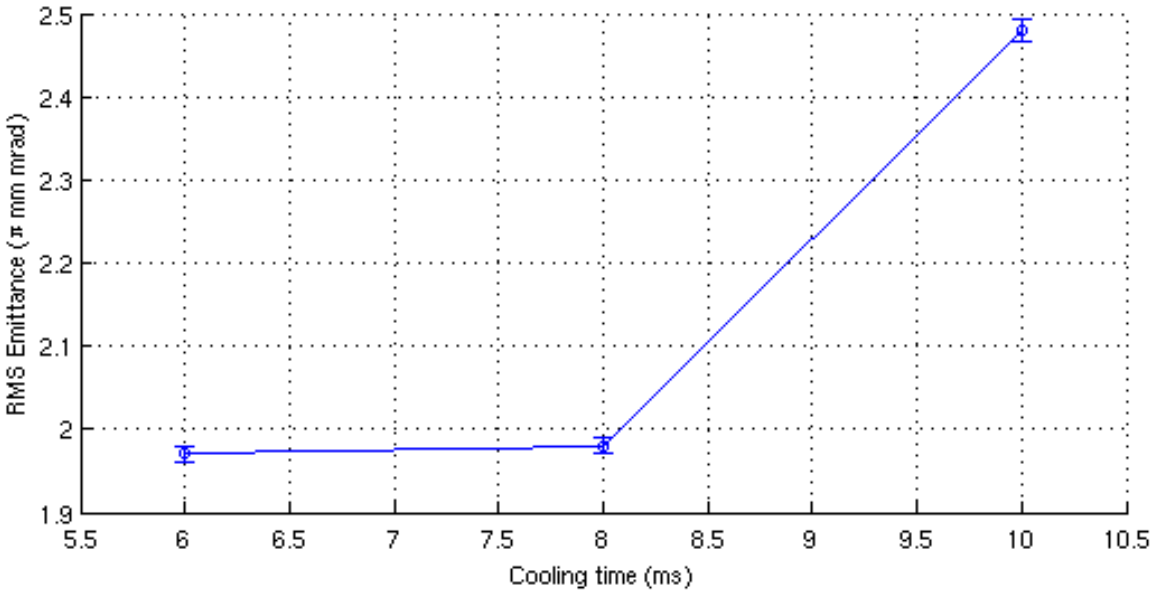

Figure 16: RMS Emittance vs. cooling time at constant gas flow of 10sccm

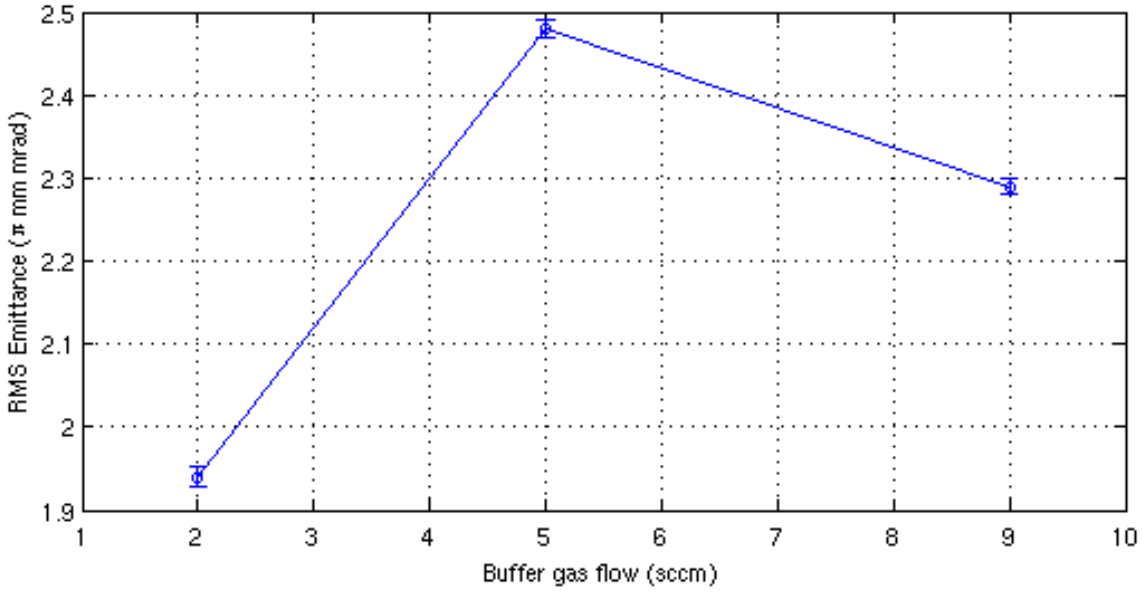

Figure 17: RMS emittance vs. gas flow at constant cooling time of 5ms

5. Conclusion

This measurement has given us good qualitative information about the behaviour of the reverse-extracted ion beam, its rough dimensions in phase space and its response to varying RFQ conditions. However, given that the measurement has a large known source of uncertainty, the quantitative aspects of the measurement are somewhat untrustworthy. Steps should be taken to eliminate this error in order to obtain a convincing value for the reverse-extracted RFQ emittance. To accomplish this, we plan to redo the measurement using a more suitable, low-voltage power-source to supply the deflector-plate potential, in hopes of eliminating the most likely cause of the emittance-plot discontinuity.

5. References

[1] M. Stockli, “Measuring and Analyzing the Transverse Emittance of Charged Particle Beams” in *Beam Instrumentation Workshop 2006: Twelfth Workshop*, American Institute of Physics, 2006, pp. 27-34.

[2] P. Allison, J. Sherman and D. Holtkamp, “An Emittance Scaner For Intense Low-Energy Ion Beams” in *IEEE Transactions on Nuclear Science, Vol. NS-30, No.4*, Los Alamos National Laboratory, 1983, p. 2204.